



A 1-km dataset of crop residue production and usage pathways in the conterminous U.S. from 2001 to 2021

Yikun Zhang¹, Hua Yan¹, Wenzhe Jiao², Yanghui Kang³, Marty R. Schmer⁴, Ryan D. Stewart¹, Benjamin F. Tracy¹, Yongfa You^{1,*}

5 ¹School of Plant and Environmental Sciences, Virginia Tech, Blacksburg, VA, USA

²Department of Ecology and Conservation Biology, Texas A&M University, College Station, TX, USA

³Department of Biological Systems Engineering, Virginia Tech, Blacksburg, VA, USA

⁴USDA-Agricultural Research Service, Agroecosystem Management Research Unit, Lincoln, NE, USA

*Correspondence to: Yongfa You (yongfayou@vt.edu)

10 **Abstract.** Crop residues represent an important biomass resource that supports soil organic carbon maintenance, livestock
production, and emerging bioeconomy sectors. In the United States, crop residue production is concentrated in a few
dominant cropping systems, whereas residue demand for livestock and other off-field uses is often geographically
separated from production regions. However, spatially explicit datasets that jointly quantify crop residue production,
allocation pathways, and spatial imbalances between production and consumption remain limited. Here, we developed a
15 1 km × 1 km gridded dataset of crop residue production and usage pathways across the conterminous United States for
2001–2021, covering nine major crops. A mass-balance framework was applied to reconcile residue production and
consumption, allocating residues into four pathways: left on field, animal-use, off-field use, and burnt. An implied
domestic transfer layer was also derived as an indicator of spatial mismatches between residue production and
consumption. Results indicate that total U.S. residue production averaged 4.91×10^{11} kg/yr, with corn residue consistently
20 contributing over 60% of the total biomass. Residues left on field dominated nationally, accounting for 86.4% of total
residue production. Livestock use and off-field uses represented smaller but spatially heterogeneous pathways (13.4%
combined), while burnt residue accounted for less than 0.2%. Residue production was concentrated in the Midwest,
whereas higher consumption demand occurred in the Southeast, West Coast, and the Southern Great Plains. The national
production-consumption mismatch ratio increased from 7.6% to 8.4% over the study period, highlighting a growing
25 spatial imbalance between residue availability and consumption demand. By providing 1-km gridded, mass-balanced
estimates of residue production, allocation pathways, and regional production-consumption mismatches, this dataset
offers a spatially explicit foundation for quantifying crop residue flows across U.S. agricultural landscapes and supports
improved representation of residue management in terrestrial biosphere models, soil carbon dynamics assessments, and
sustainable residue biomass utilization strategies. The dataset is available at <https://doi.org/10.5281/zenodo.18453064>
30 (Zhang et al., 2026).



1 Introduction

Crop residues, the non-harvested fraction of crop aboveground biomass, play a critical role in regulating agroecosystem functioning and sustainability (Baloch et al., 2025). When retained on the field, residues provide organic matter inputs that support soil organic carbon (SOC) accumulation, sustain microbial activity, and improve soil physical conditions such as water retention, thermal buffering, and erosion resistance (Baloch et al., 2025; Fu et al., 2021; Ranaivoson et al., 2017). Through these processes, residue retention influences both short-term crop performance and long-term soil function (Lal, 1995; Smil, 1999). At the same time, crop residues are an economically valuable biomass resource widely used for livestock feed and bioenergy production (Krishna and Mkondiwa, 2023), contributing to spatially heterogeneous residue usage patterns and potentially introducing competing demands between soil conservation and off-field uses (van Selm et al., 2025; Tifton et al., 2015). However, spatially explicit data on crop residue pathways remain limited across agricultural landscapes (Schmer et al., 2017; Smerald et al., 2023). In the absence of such data, terrestrial biosphere models typically rely on simplified assumptions such as fixed residue removal fractions, which introduce substantial uncertainty in simulated SOC dynamics and land-atmosphere carbon exchange (Anand et al., 2022; Pongratz et al., 2018). Addressing these data limitations is essential for advancing our understanding of how residue management influences soil function, crop productivity, and biogeochemical cycling.

A growing body of research has quantified crop residue production at regional to global scales using statistical data and modeling approaches (Daioglou et al., 2016; Jiang et al., 2012; Scarlat et al., 2010), providing important estimates of residue availability but offering limited insight into subsequent usage pathways such as residue retention, removal, or alternative uses. More recent studies have expanded toward residue management using surveys, modeling approaches, or data synthesis (Schmer et al., 2017; Zhang et al., 2025). However, many remain limited to localized regions or rely on aggregated statistics at county to state scales, which obscure fine-scale management variability. Additionally, most existing work does not explicitly integrate estimates of residue production and consumption within a spatially explicit, mass-balanced framework, resulting in inconsistencies between residue supply and demand and limiting the ability to trace residue flows across fields and downstream users. A recent global dataset partitioned residue production into multiple usage pathways, including livestock feed, burning, and other off-field uses (Smerald et al., 2023). This dataset provides an important basis for large-scale assessments, but its relatively coarse spatial resolution (0.5°) and regionally aggregated allocation parameters may limit the representation of sub-grid variability and local landscape characteristics. As a result, fine-scale variability in residue usage pathways remains poorly resolved in existing datasets.

In the United States (U.S.), annual crop residue production is nearly 5×10^{11} kg, accounting for about 13% of the global total (Lal, 1995; Smerald et al., 2023). Residue production is dominated by a small number of major cropping systems, particularly corn, soybean, and wheat, resulting in strong regional concentration of biomass supply (Ye et al., 2024). In contrast, livestock-intensive regions in the U.S. are often geographically separated from major crop production areas, creating structural imbalances between residue availability and off-field demand for feed and other uses (Schmer et al., 2017; Sulc and Tracy, 2007). This geographic separation implies substantial interregional redistribution of residues, yet



65 the magnitude and spatial pattern of such production-consumption mismatches remain poorly quantified. Residue
allocation is further shaped by regionally specific management practices and policy contexts, including conservation
programs, tillage systems, and burning regulations (de Camargo Santos et al., 2025; McCarty et al., 2009; Muth et al.,
2013). There is a need for a spatially explicit dataset that simultaneously links residue production, multiple utilization
pathways, and implied transfer in the U.S., which can be used to quantify regional residue flows and identify opportunities
70 for sustainable residue management.

Here we present a 1 km × 1 km gridded dataset of crop residue production and usage pathways across the conterminous
U.S. from 2001 to 2021. The dataset covers nine major crops, including barley, corn, cotton, rice, sorghum, soybean,
durum wheat, spring wheat, and winter wheat, and allocates residues into four pathway categories: burnt, animal-use, off-
field use, and left on field. By linking residue production with spatially explicit pathway allocation under a mass-balanced
75 framework, the dataset provides a consistent representation of residue usage and flows across U.S. croplands. We also
release an implied domestic transfer layer that identifies locations where spatial redistribution is required to reconcile
residue production and consumption, providing additional insights into regions with potential supply-demand mismatch.
This dataset provides a national-scale benchmark for quantifying residue flows and improving representation of residue
dynamics in SOC modeling, as well as supporting more effective and sustainable management of crop residues.

80 **2 Methodology**

2.1 Datasets

Multiple raster and inventory datasets were compiled to quantify crop residue production and usage pathways across the
conterminous U.S. (Table 1):

(1) Residue production: County-level crop yield and harvested area data for nine major crops were obtained from the
85 USDA-National Agricultural Statistics Service (USDA-NASS) to estimate crop production and associated residue
production. The CropAT-US dataset, providing 1-km crop-specific distribution fractions across the conterminous U.S.
(Ye et al., 2024), was used to derive grid-level residue production.

(2) Burnt residue: Burned-area observations were obtained from the MODIS/VIIRS MCD64A1 product at 500 m spatial
resolution. Crop-specific planting and harvesting calendars from the USDA were collected to extract fire events
90 specifically within crop-specific harvest windows, thereby excluding non-agricultural biomass burning.

(3) Animal-use residue: Livestock distribution data was obtained from a 5 km gridded livestock density dataset (Du et
al., 2025), together with county-level livestock statistics from the USDA Census of Agriculture, to estimate livestock-
associated residue use.

(4) Off-field residue: International trade records of cereal straw and husks were obtained from the World Integrated Trade
95 Solution (WITS) database to describe national-level biomass transfers associated with off-field residue use. A global 5



arc-minute gross domestic product (GDP) raster (Kummu et al., 2025) was included as a socioeconomic proxy for local industrial activity linked to other domestic off-field uses.

Table 1. Summary of primary spatial and statistical data sources

Category	Data content	Data type/resolution	Data source
Residue production	CropAT-US dataset	Raster, 1 km	https://doi.org/10.5194/essd-16-3453-2024
	USDA-NASS crop yield and harvest area data	Inventory	https://quickstats.nass.usda.gov/
Burnt residue	MODIS/VIIRS burned-area products (MCD64A1)	Raster, 500 m	https://ladsweb.modaps.eosdis.nasa.gov/missions-and-measurements/products/MCD64A1/
	USDA Usual Planting and Harvesting Dates for U.S. Field Crops	Inventory	https://esmis.nal.usda.gov/sites/default/release-files/vm40xr56k/dv13zw65p/w9505297d/planting-10-29-2010.pdf
Animal-use residue	Gridded livestock data	Raster, 5 km	https://doi.org/10.5194/essd-17-5543-2025
	USDA-NASS county-level livestock census data	Inventory	https://quickstats.nass.usda.gov/
	USDA-NASS national beef production data	Inventory	https://quickstats.nass.usda.gov/
Off-field residue	International trade statistics (WITS)	Inventory	https://wits.worldbank.org/trade/comtrade/en/country/ALL/year/2024/tradeflow/Exports/partner/WLD/product/121300
	GDP raster dataset	Raster, 5 arcmin	https://doi.org/10.1038/s41597-025-04487-x

Note: Unless otherwise stated, all datasets were compiled for 2001–2021. USDA livestock census data (1997–2022) were used to support interpolation in non-census years. All raster datasets were resampled to 1-km resolution.

2.2 Methodology framework

2.2.1 Logical framework and workflow

Our dataset was developed based on a mass-balance framework that divides total residue production (P) into four pathways: burnt (B), local animal use (A), off-field use (O) (including outflow to other areas), and residue left in the field (L) (Figure 1). Total residue production was first estimated at grid-level for nine major crops to quantify residue availability (Step 1). Consumption-based residue demand, including burnt residue, animal-use demand, and off-field use, was then quantified to represent major residue removal processes (Step 2). Because residue demand within individual grid cells may exceed locally generated residue production, residues were redistributed across grids under a mass-balance constraint to conserve total quantities, generating an implied domestic transfer layer that represents spatial redistribution between residue surplus and deficit regions (Step 3). The redistributed residue quantities were subsequently allocated into four pathways, including burnt, animal-use, off-field, and residue left on the field (Step 4).

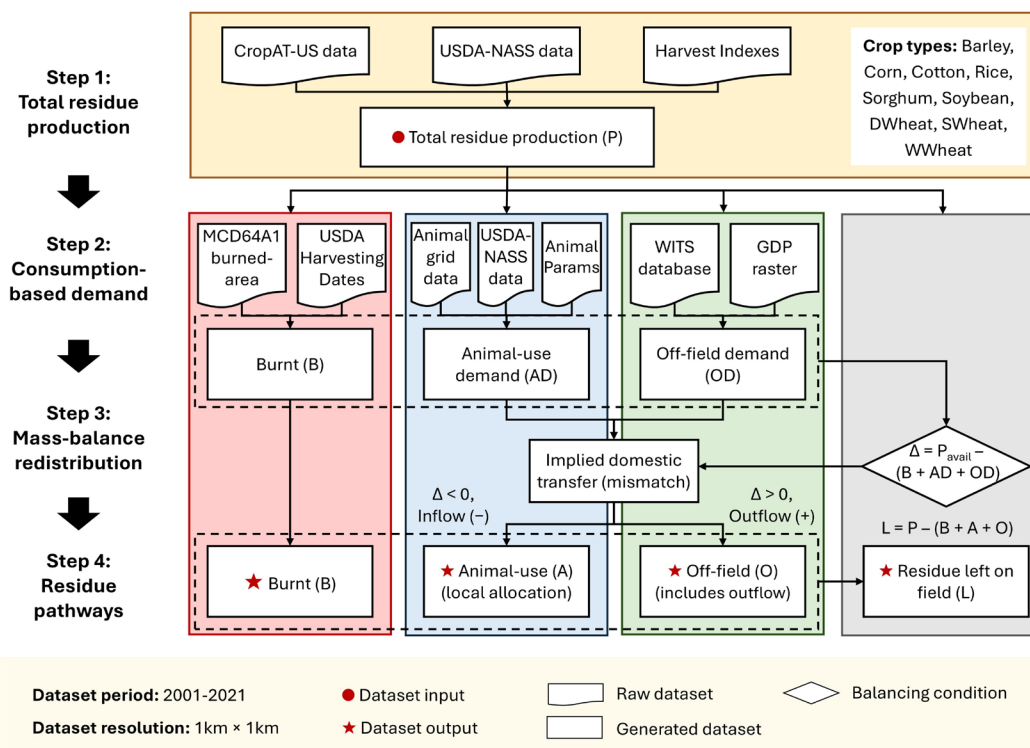


Figure 1. Workflow of the crop residue production and usage pathway framework. The consumption-based burnt residue is directly retained as the burnt pathway. P_{avail} denotes the maximum available residue at the grid level and is set to 90% of the total residue following Smerald et al. (2023). DWheat, SWheat, and WWheat refer to durum wheat, spring wheat, and winter wheat, respectively. We define implied domestic transfers as the mass-balance redistribution required to reconcile spatial mismatches between residue production and consumption; inflow and outflow represent inferred domestic deficit and surplus redistribution during reconciliation and are distinct from international export, which is quantified independently from statistics.

2.2.2 Total residue production calculation

Total residue production was quantified for nine major crops: barley, corn, cotton, rice, sorghum, soybean, durum wheat, spring wheat, and winter wheat. County-level grain yield statistics from 2001 to 2021 were obtained from the USDA-NASS. Crop-specific distribution fractions from the CropAT-US dataset (Ye et al., 2024) were used to downscale county-level crop yields to 1 km² grid cells by representing each crop's within-county spatial distribution. Grid-level grain yield was then calculated as the crop-area-weighted mean of crop-specific yields, normalized by the summed crop fraction within each grid cell. Missing values in the USDA-NASS yield inventory were filled using county-specific yield regressions developed from available historical data. The resulting grid-level grain yields were converted to residue biomass production using crop-specific, time-dependent harvest indices (HI , Table 2), which account for temporal changes in crop genetic improvement and agricultural management practices. The relationship between residue production (P), grain yield (Y), and HI is expressed as:



130

$$P = Y \times \left(\frac{1}{HI} - 1 \right) \quad (1)$$

Note: HI denotes harvest index (dimensionless) as a function of calendar year (Year).

Table 2. Harvest index of each crop in the U.S.

Crop Type	Equation	References
Wheat (durum, spring, winter)	$0.32 + \frac{0.22}{1 + \exp(-0.08 \times (\text{Year} - 1955))}$	Lu et al. (2018); Haberl et al. (2001); Allmaras et al. (2000)
Sorghum	$0.31 + \frac{0.20}{1 + \exp(-0.10 \times (\text{Year} - 1955))}$	Lu et al. (2018); Haberl et al. (2001); Allmaras et al. (2000)
Barley	$0.24 + \frac{0.16}{1 + \exp(-0.10 \times (\text{Year} - 1955))}$	Lu et al. (2018); Haberl et al. (2001); Allmaras et al. (2000)
Corn, soybean, rice	$0.47 \times \frac{1 + 0.65 \times (\tanh(\text{Year} - 2000))}{70}$	Lu et al. (2018); Zeng et al. (2014)
Cotton	0.47	Wanjura et al. (2012)

2.2.3 Residue usage pathways synthesis

2.2.3.1 Burnt residue

135 Burnt residue refers to crop biomass removed through open-field burning after harvest. Burned area observations were
 obtained from the 500 m MODIS/VIIRS burned-area product (MCD64A1) and combined with CropAT-US crop
 distribution maps and USDA Usual Planting and Harvesting Dates to identify burning events occurring within croplands
 during crop-specific harvest windows (Table 1). Because residue burning may occur after harvest and the USDA harvest
 dates represent broad state-level windows, burned-area detections within these windows were attributed to post-harvest
 140 residue burning. Burnt residue was estimated following Wiedinmyer et al. (2023):

$$B_i(x, t) = BA_i(x, t) \times BP_i(x, t) \times FB_i \quad (2)$$

where $B_i(x, t)$ is the burnt residue for crop type i at location x and time t , $BA_i(x, t)$ is the burned area, $BP_i(x, t)$ is the
 residue biomass production, and FB_i is the crop-specific fraction of biomass burned. FB_i was set to 0.9 for corn and
 wheat (durum, spring, and winter wheat) and 0.8 for other crop types (Eggleston et al., 2006). Annual grid-level FB
 145 values were capped at 0.9 to avoid double counting from multiple fire detections at the same location.

2.2.3.2 Animal-use residue

The animal-use pathway represents crop residues utilized locally for livestock feeding and bedding, excluding any implied
 domestic inflow required to satisfy local deficits. Five animal types, including cattle, horses, sheep, goats, and pigs, were
 considered as the primary residue-consuming animals in the U.S. (Hristov et al., 2014; Smerald et al., 2023).
 150 Animal-use residue demand (AD) was estimated as the consumption-based residue required by livestock populations
 regardless of local residue supply (Figure 1). This demand was estimated by integrating spatialized livestock densities



with species-specific parameters. Specifically, livestock densities were derived by downscaling gridded livestock data (Du et al., 2025) and calibrating against USDA-NASS county-level livestock statistics. Linear interpolation was employed in inter-censal years in USDA-NASS statistics to maintain temporal continuity. The resulting livestock distributions were then converted to residue demand using species-specific bedding and feeding parameters (Table 3). For beef cattle, residue demand was modeled under four scenarios (S_0 , S_L , S_M , and S_H) in feed conversion ratios (FCR) and crop residue feed fractions (CRFF) to account for management uncertainties.

To account for spatial mismatches between livestock demand and residue production, we applied a mass-balance reconciliation (Section 2.2.4) to partition the initial AD into a locally satisfied portion (A) and a deficit requiring domestic inflow (D). The reconciled animal-use pathway is therefore expressed as:

$$A(x, t) = AD(x, t) - D(x, t) \quad (3)$$

where $A(x, t)$ is reconciled animal-use pathway at location x and time t , AD is consumption-based livestock residue demand, and D is the implied domestic inflow (deficit) at the grid level. The derivation of D based on mass-balance reconciliation is detailed in Section 2.2.4.

Table 3. Key parameters for estimating animal residue demand for feeding and bedding

Animal	Scenarios	Feeding demand		Bedding demand (kg/head/year)	References
		FCR	CRFF		
Cattle	Beef cattle	Zero feeding (S_0)	N/A	0	Herrero et al. (2013)
	Low feeding (S_L)	6	0.12	136.9	USDA Economic Research Service (2026), Herrero et al. (2013)
	Medium feeding (S_M)	14.3	0.23		Peters et al. (2014), Herrero et al. (2013)
	High feeding (S_H)	25	0.35		Mekonnen and Hoekstra (2012), Herrero et al. (2013)
Dairy cattle	All scenarios	0		136.9	Smerald et al. (2023)
Horse	All scenarios	420 kg/head/year		547.5	Smerald et al. (2023)
Sheep	All scenarios	0		36.5	Smerald et al. (2023)
Goat	All scenarios	0		36.5	Smerald et al. (2023)
Pig	All scenarios	0		22.8	Smerald et al. (2023)

2.2.3.3 Off-field residue

The off-field pathway represents residues removed from the production site for purposes other than local animal husbandry. This pathway was quantified by integrating consumption-based off-field demand (OD) with regional outflows from surplus grid cells (Figure 1).

The OD term was further divided into international net exports and other domestic uses (Table 1). International net export volumes were derived from the WITS database and calibrated against the U.S. cereal straw and husks exports and imports records. Other domestic uses encompass activities such as traditional fuel consumption and mushroom cultivation, for which spatially explicit statistics are limited. We therefore assumed a national baseline of approximately 1% of total



175 residue for these uses, consistent with the ranges reported in the literature (Krishna and Mkondiwa, 2023; Smerald et al., 2023). To reflect regional socioeconomic variations, this fraction was differentiated using per capita GDP as a proxy. Specifically, low-income regions were assigned a higher utilization intensity (up to 5%) due to their continued dependence on traditional biomass for household energy, while high-income regions were assumed to have transitioned to modern residential energy systems, leading to near-zero localized use (Smerald et al., 2023).

180 In addition to OD , the off-field pathway includes domestic outflow from surplus grid cells identified through mass-balance reconciliation (Section 2.2.4). Therefore, the reconciled off-field pathway is calculated as:

$$O(x, t) = OD(x, t) + F_{out}(x, t) \quad (4)$$

where $O(x, t)$ is reconciled off-field residue pathway, OD is consumption-based off-field demand, including international net exports and other domestic off-field uses, and F_{out} is the implied domestic outflow from surplus grid cells. The derivation of F_{out} based on mass-balance reconciliation is detailed in Section 2.2.4.

185 2.2.3.4 Residue left on field

Residue left on field represents crop residues retained on the production site to support soil functions and erosion control. In this study, residue left on field was calculated as the residual biomass after subtracting the burnt, animal-use, and off-field pathways from the total aboveground residue production (Figure 1):

$$L(x, t) = P(x, t) - (B(x, t) + A(x, t) + O(x, t)) \quad (5)$$

190 where L , P , B , A , and O are residue left on field, total residue production, burnt residue, animal-use residue, and off-field residue, respectively.

2.2.4 Mass-balance residue redistribution

A mass-balance residue redistribution was applied to reconcile spatial discrepancies between residue production and consumption at the grid level. Following a commonly used retention assumption, the maximum available production
195 P_{avail} was capped at 90% of total residue production (P) (Smerald et al., 2023).

$$P_{avail}(x, t) = 0.9 \times P(x, t) \quad (6)$$

Grid cells where the sum of consumption-based demand (i.e., burnt residue, animal-use residue demand, and off-field residue demand) exceeded P_{avail} were categorized as “domestic inflow” areas (D, deficit), while grids with demand below P_{avail} were identified as “domestic outflow potential” areas (S, surplus).

$$200 \quad D(x, t) = \max(0, B(x, t) + AD(x, t) + OD(x, t) - P_{avail}(x, t)) \quad (7)$$

$$S(x, t) = \max(0, P_{avail}(x, t) - (B(x, t) + AD(x, t) + OD(x, t))) \quad (8)$$

where P_{avail} is the maximum available production, B is burnt residue, AD is animal-use demand, OD is off-field demand, and D and S mean deficit or surplus (kg per grid cell per year), respectively.



To ensure mass balance, the total required inflow was proportionally allocated across surplus grids. Specifically, an
205 outflow ratio (r) was calculated by dividing the total domestic inflow (D) by the total outflow potential (S), which was
then applied to determine the actual outflow (F_{out}) from each surplus grid.

$$r(t) = \frac{\sum_x D(x, t)}{\sum_x S(x, t)} \quad (9)$$

where $r(t)$ is the outflow ratio at time t .

$$F_{out}(x, t) = r(t) \cdot S(x, t) \quad (10)$$

210 where $F_{out}(x, t)$ is the actual outflow at location x and time t . The national sum of F_{out} equals to the sum of D , ensuring
mass balance at year t . This proportional redistribution does not reflect actual transportation flows but instead represents
a conceptual reallocation required to maintain mass balance.

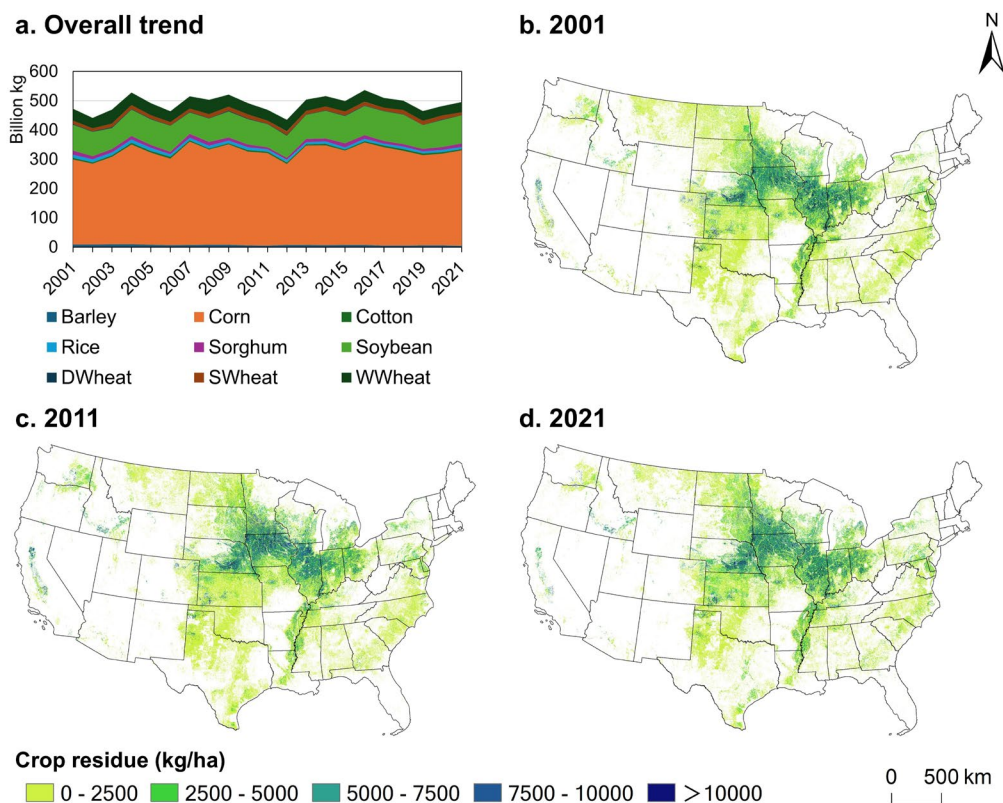
2.3 Evaluation and consistency validation

The generated dataset was assessed across three aspects: (1) National-level comparison: national-level aggregated residue
215 production was compared with official statistics and published literature. (2) Pathway-specific evaluation: usage-specific
pathways were evaluated by comparing calculated residue management ratios with values reported in previous studies
and available survey-based evidence. (3) Spatial consistency: spatial patterns were qualitatively compared with an
existing global crop residue dataset.

3 Results

220 3.1 Total crop residue production dynamics

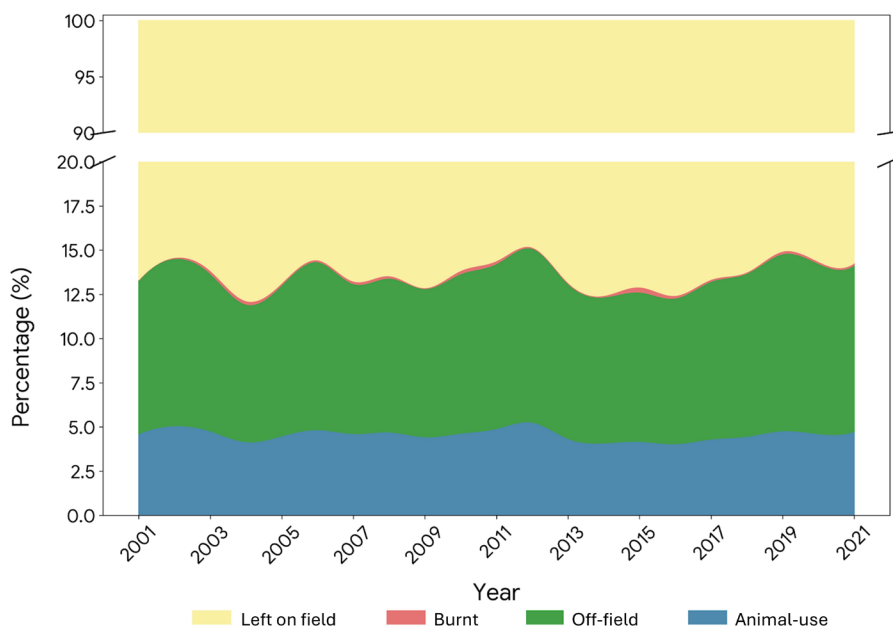
From 2001 to 2021, total crop residue production in the U.S. remained relatively stable, with annual production ranging
from 4.41×10^{11} kg to 5.37×10^{11} kg (Figure 2a). Corn residue consistently dominated the national residue supply,
accounting for over 60% of total residue, followed by soybean and winter wheat (Figure 2a). The geospatial distribution
of residue production exhibited a consistent pattern over the past two decades (Figure 2b-d). High-production areas were
225 concentrated in the Midwest (the Corn Belt) and the Mississippi River Basin, where residue production exceeded 7500
kg/ha in many locations. Conversely, low-production areas concentrated in the Pacific coast and the northeast U.S.
Although the overall national distribution remained stable, residue production density in parts of Kansas and Texas
slightly increased, while the density in California's Central Valley slightly decreased (Figure 2b, d).



230 **Figure 2.** Spatiotemporal patterns of total crop residue production in the U.S. (a) Temporal trends in annual residue production by crop
(unit: billion kg), where DWheat, SWheat, and WWheat denote durum wheat, spring wheat, and winter wheat, respectively; (b-d)
235 Spatial patterns of total residue production across the U.S. in 2001, 2011, and 2021, respectively (unit: kg/ha). The crop-specific residue
production distribution is provided in Figures S1.

3.2 Crop residue usage pathways dynamics

235 Crop residue usage pathways exhibited relatively stable yet uneven patterns from 2001 to 2021 (Figure 3). Residue
retention (left on field) dominated the residue pathway, accounting for 86.4% on average of total residue production.
Among the remaining pathways, off-field use represented the largest secondary share, ranging between 8% and 10% of
residue production. The animal-use pathway remained relatively stable, fluctuating between 4% and 5%, whereas burnt
residue constituted only a minimal fraction, contributing less than 0.2% of total national residue production.

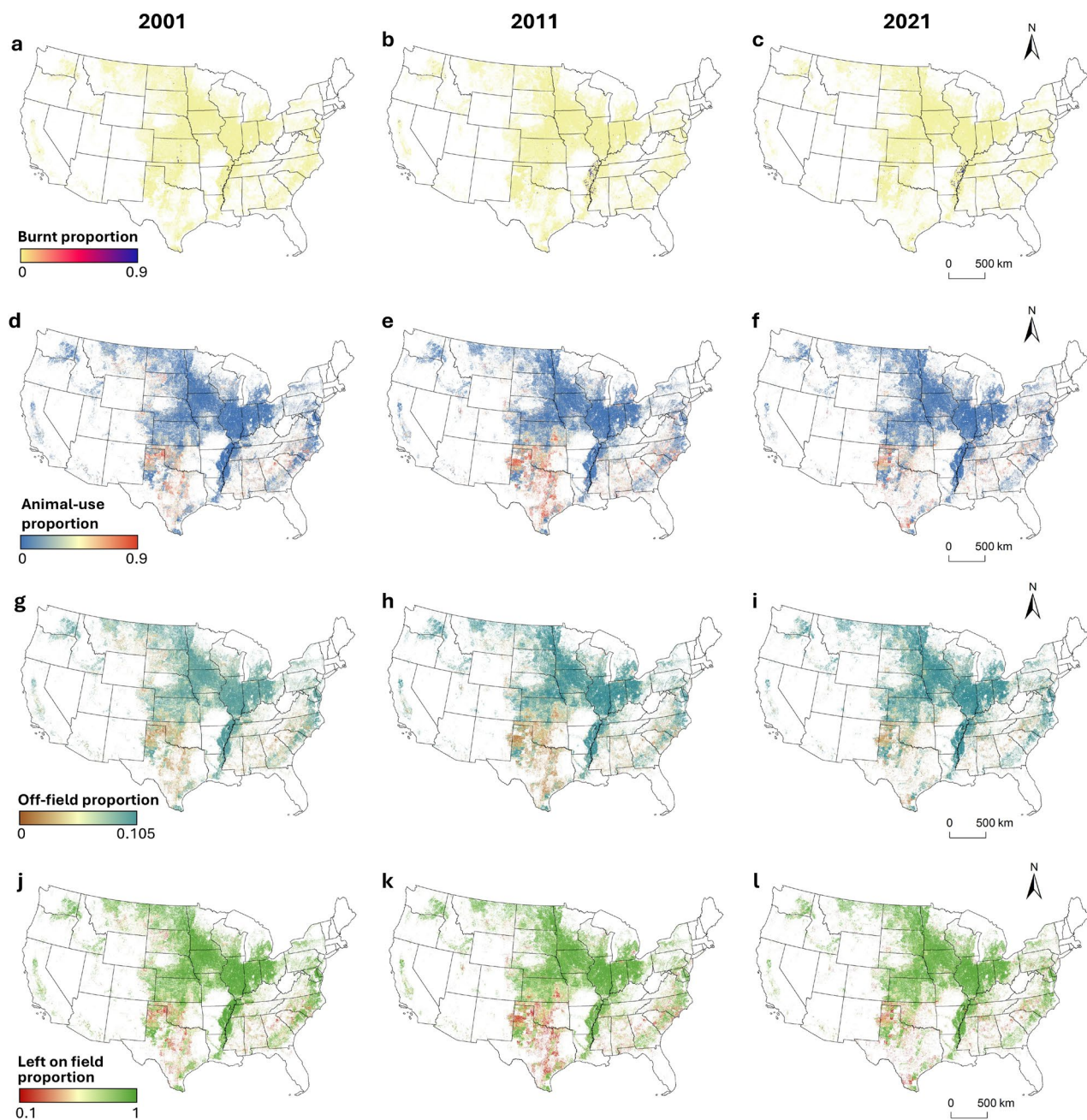


240

Figure 3. Temporal variation in residue pathway proportions. The animal-use pathway only includes local use (i.e., domestic inflow excluded), and the off-field pathway includes international net export, domestic outflow, and other domestic off-field uses. Unless otherwise stated, all values shown represent the arithmetic mean across the four scenarios (S₀–S_H).

245 The spatial distribution of crop residue usage pathways showed strong heterogeneity across the U.S. (Figure 4). Burnt residue was spatially scattered, with hotspots concentrated in the Mississippi River Delta region (Figure 4a-c). The animal-use pathway was more prevalent in the southern states and the Great Plains, where grazing and animal husbandry are common (Figure 4d-f, S9). The off-field pathway accounted for a relatively small proportion nationally but showed a clear geographic expansion, particularly across the Midwest and the Mississippi River basin; however, grid-level proportions generally remained below 10% (Figure 4g-i). Most crop residues were retained on the field, with higher retention in the Midwest, aligning with major high-yield production areas (Figure 4j-l).

250

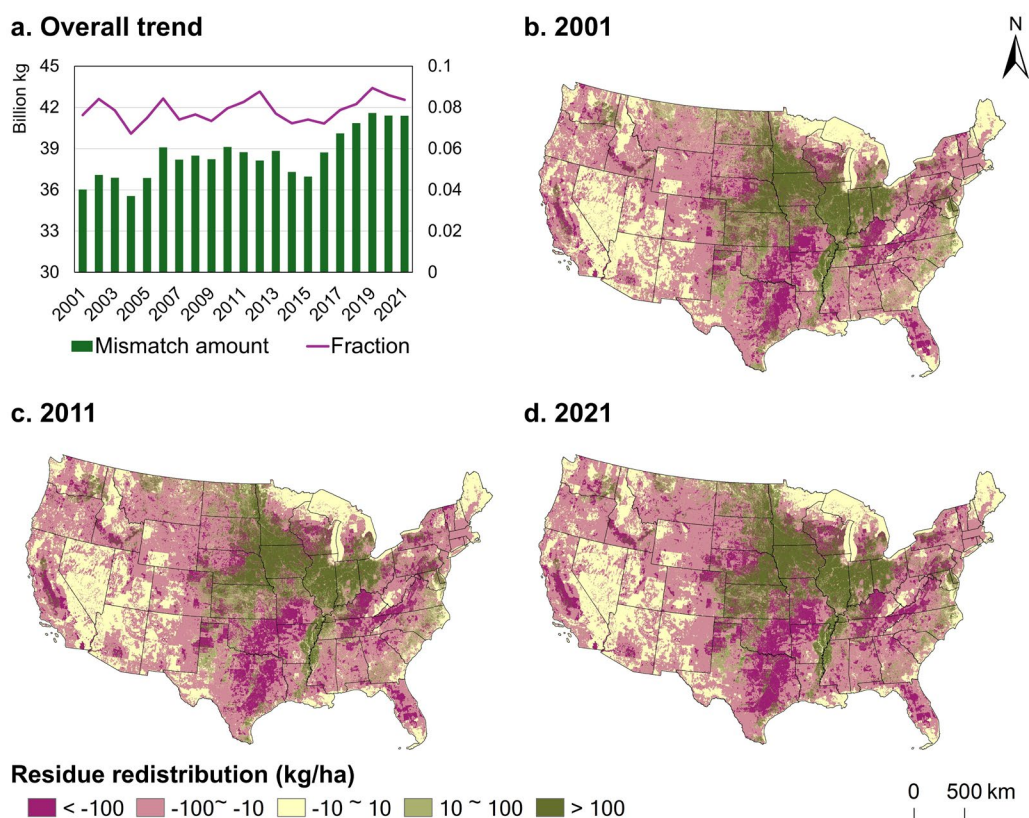


255 **Figure 4.** Spatial patterns of crop residue pathway proportions in 2001, 2011, and 2021. (a–c) Burnt residue proportion, (d–f) animal-use residue proportion (local allocation), (g–i) off-field residue proportion (including international net export, domestic outflow, and other domestic off-field uses), and (j–l) residue left on field proportion. All proportions are relative to total residue production in each grid cell. Unless otherwise stated, all values shown represent the arithmetic mean across the four scenarios (S₀–S_H). The scenario-specific residue demand and usage pathways distribution are provided in Figures S2–S4, S6–S8.



3.3 Residue production-consumption mismatch

The national mismatch between residue production and consumption intensified from 2001 to 2021 (Figure 5). The mismatch amount (defined as the sum of absolute implied inflow or outflow) increased from 3.60×10^{10} kg to 4.14×10^{10} kg over two decades, with its relative share of total residue production rising from 7.6% to 8.4% (Figure 5a). The spatial distribution of residue transfers exhibited a distinct geographic structure in terms of sources versus sinks. The Midwest served as the major outflow region (green areas), where available residue production consistently exceeded local demand. In contrast, the Southeast, the West Coast, and the Southern Great Plains emerged as major inflow regions (purple areas), where demand exceeded locally available residue production (Figure 5b-d). Notably, the redistribution intensity within these core regions also increased over time. By 2021, the spatial footprint of high-intensity transfers (absolute values >100 kg/ha) had expanded significantly compared to 2001, indicating a greater spatial separation between residue production and consumption and an increasing residue transfer across regions (Figure 5d).



270 **Figure 5.** Spatiotemporal patterns of residue production-consumption mismatch and redistribution. (a) Annual mismatch amount (billion kg; defined as the sum of absolute inflow or outflow) and mismatch fraction (fraction of total residue production) during 2001–2021; (b-d) Spatial patterns of residue redistribution across the U.S. in 2001, 2011, and 2021 (unit: kg/ha). Unless otherwise stated, all values shown represent the arithmetic mean across the four scenarios (S_0 – S_{II}). The scenario-specific residue production-consumption mismatch is provided in Figure S5.



275 **Note:** Redistribution is inferred from grid-level mass-balance reconciliation and represents domestic reallocation required to align consumption with production. Negative values indicate inflow (local consumption exceeds available production, $P_{avail}=0.9P$), positive values indicate outflow (local available production exceeds local consumption).

4 Discussion

4.1 Dataset validation

280 The estimated national crop residue production of 4.91×10^{11} kg/yr ($4.41 - 5.37 \times 10^{11}$ kg/yr) falls within the range reported in previous U.S. national studies, which varied from 4.88×10^{11} kg/yr to 6.52×10^{11} kg/yr (Table 4). While our estimation aligns well with localized U.S. studies (Chatterjee, 2013; Lal, 2005), our inventory covers a broader scope than recent global cereal-focused products. By incorporating key non-cereal crops such as soybean and cotton, our estimate is therefore higher than the North American cereal residue production reported by Smerald et al. (2023) (4.60×10^{11} kg/yr).
285 Conversely, the higher estimate from Sileshi et al. (2025) (6.52×10^{11} kg/yr) may be partly attributable to their use of the FAOSTAT dataset, which may overestimate cropland area (Yu and Lu, 2018). Our study is anchored to the high-resolution CropAT-US distribution data, which helps to reduce this bias (Ye et al., 2024). Moreover, integrating time-dependent HI refines the representation of residue production dynamics, providing a more accurate estimation of residue availability than the static coefficients commonly used in coarse-resolution global studies.
290 Our dataset of crop residue usage pathways also aligns with the established U.S. hierarchy, in which residue left on field represents the dominant pathway, followed by animal-use and off-field pathways, with burning representing a much smaller loss pathway (Figure 3, Table 4). Although the overall hierarchy is consistent with national trends, the specific proportions differ from global estimates. For instance, in this study, the residue left on field rate had a mean of 86.4%, which is higher than the reported average (~76.2%) (Table 4). While global models typically cap North American return rates at 80% (Smerald et al., 2023), U.S.-specific surveys indicate that residue removal is not a widespread practice. Corn provides a representative example due to its high biomass utilization potential in the U.S.; however, ground surveys reveal that only about 14-16% of corn acres undergo residue-removing practices such as harvest or grazing, implying that the majority of U.S. croplands maintain high residue retention levels (Claassen et al., 2018; Schmer et al., 2017). Our estimated burning rate (<0.2%) is lower than previous estimates (which ranged from 1-2%) (Table 4), partly due to the
295 finer spatial resolution in our study. Previous studies often relied on coarse-resolution fire datasets (e.g., 0.5° and 0.25°) (Smerald et al., 2023), whereas our approach uses 1-km resolution data and restricts fire events to crop-specific harvest windows, which reduces the likelihood of including non-agricultural biomass burning in cropland pixels.
300



Table 4. Comparison of U.S. crop residue production and usage pathways with existing literature

Source	Scope	Total production (10 ¹¹ kg/yr)	Residue left on field (%)	Burnt residue (%)
This Study	U.S. (Multi-crop, 1 km)	4.91	86.4%	0.1%
Smerald et al. (2023)	North America (Cereals)	4.60	~76.2%	~1.8%
Sileshi et al. (2025)	U.S. (Multi-crop)	6.52	N/A	N/A
Chatterjee (2013)	U.S. National	5.18	N/A	N/A
Lal (2005)	U.S. National	4.88	N/A	N/A
Claassen et al (2018)	U.S. (Corn stover)	N/A	~84% (area)	N/A
Schmer et al (2017)	19 States of U.S. (Corn stover)	N/A	~86% (area)	N/A
McCarty et al. (2009)	U.S. (Multi-crop)	N/A	N/A	~1% (area)

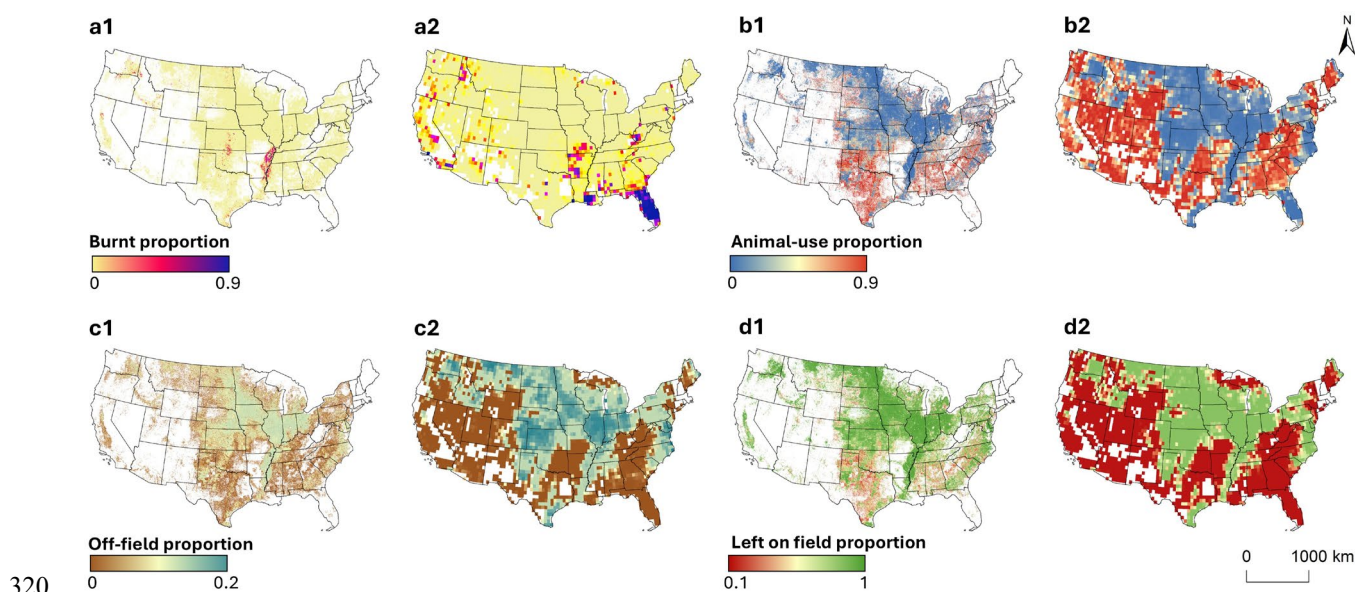
Note: Values marked as “area” are reported as area fractions (i.e., the percentage of cropland area where residues are managed under a given pathway), whereas other values represent mass fractions (i.e., the percentage of total residue mass allocated to that pathway). Area- and mass-based fractions are not directly comparable because residue production per unit area varies spatially. The limited availability of studies reporting comparable metrics highlights the need for consistent, spatially explicit pathway datasets.

305

310

315

The spatial distribution of our dataset also demonstrates high geospatial consistency with established global patterns, with only minor discrepancies (Figure 3, Figure 6). For instance, one notable difference appears in Florida, where the burnt proportion is lower in our dataset (Figure 6a1, 6a2). This contrast mainly results from differences in crop coverage. While Smerald et al. (2023) aggregated sugarcane, which accounts for the majority of burning activities in Florida, this crop is not included in our dataset. Additionally, due to resolution difference, our dataset exhibits a more heterogeneous spatial footprint than the global product (Figure 6). The 0.5° resolution of global products often fails to resolve sub-pixel land cover variations; consequently, fire events in these coarse pixels may be insufficiently distinguished from crop residue burning even when only a fraction of the area is cropland. In contrast, our 1-km dataset captures cropland pixels more explicitly. Consequently, our dataset provides a more targeted representation of residue pathway, reducing the influence of non-agricultural land within coarse-grid cells.



320

Figure 6. Spatial comparison of multi-year average crop residue pathway proportions in the U.S. (2001–2021). Panels a1, b1, c1, d1 show the proportions (burnt, animal-use, off-field, and left on field, respectively) derived from this study at a 1-km resolution. Panels a2, b2, c2, d2 show the corresponding proportions from a global dataset with a 0.5° resolution (Smerald et al., 2023). Panels within each row share the same color scale. Unless otherwise stated, all values shown represent the arithmetic mean across the four scenarios (S₀–S_H).

325

4.2 Dataset applications

High-resolution quantification of residue inputs into soils is essential for improving the accuracy of terrestrial carbon budget estimations. Conventional SOC or terrestrial biosphere models often rely on generalized assumptions, such as uniform or fixed residue left-on-field ratios; however, these assumptions mask significant spatial heterogeneity in residue retention driven by regional resource availability, livestock demand, and market incentives (Karstens et al., 2022; Lehmann et al., 2020; Tian et al., 2015). Furthermore, SOC sequestration is determined not only by the quantity of residue inputs but also by conversion efficiency, which is highly sensitive to microbial activity, soil properties, and local climate conditions that vary at fine spatial scales (Gutierrez et al., 2023; Natalio et al., 2024). Aggregating residue inputs into coarse averages therefore creates a spatial mismatch with these localized environmental and management drivers, leading to biased estimates of carbon sink potential (Keel et al., 2017). By providing residue pathways at 1-km resolution, our dataset enables the precise alignment between residue management practices and environmental conditions, supporting more spatially explicit assessments of SOC dynamics and residue retention benefits.

330

335

Beyond SOC maintenance, crop residues connect multiple components of the U.S. bioeconomy by facilitating biomass and nutrient flows across sectors. In parts of the Great Plains and the western Corn Belt, especially in mixed crop-livestock systems, crop residues are used as feed or bedding for livestock, and nutrients contained in these residues are partially

340



returned to cropland through manure application, enhancing agroecosystem resilience (Farias et al., 2025; Russelle et al., 2007; Wang et al., 2024). However, this integration is uneven across the U.S. By mapping the spatial intensity of crop residues allocated to livestock use at 1-km resolution, our dataset identifies regions where these crop-livestock interactions are most concentrated. Such spatially explicit information provides an empirical basis for assessing the degree of regional
345 crop-livestock integration and for modeling the associated economic and environmental trade-offs (Delandmeter et al., 2025; Taifouris and Martín, 2022; Xing et al., 2022). Furthermore, our estimations of off-field residue use provide a baseline for assessing the theoretical potential of residue mobilization beyond current livestock and soil return demands. This allows more realistic assessments of where residues could support other industries (e.g., bioenergy) without compromising soil health or livestock systems (Krishna and Mkondiwa, 2023; Röder et al., 2022).

350 Another key insight from this dataset is the significant spatial mismatch between residue production and consumption, which underscores a geographical decoupling of residue supply and demand centers that had remained obscured in previous studies. While this decoupling remains modest at the national level between 2001 and 2021, the total spatial decoupling reaches 8.5×10^{10} kg under the S_H scenario, highlighting significant subnational redistribution demands (Figure 5, Figure S5, Table S2). By quantifying this supply-demand mismatch, our dataset offers a baseline for subsequent
355 economic modeling and logistics optimization (Garvie et al., 2024; Krishna and Mkondiwa, 2023; Smerald et al., 2023). Bridging these imbalances would necessitate long-distance transportation, which escalates both economic costs and the associated carbon footprint, partially offsetting the environmental benefits of residue utilization (Holmatov et al., 2021; Umakanth et al., 2022). More critically, severe local mismatches may incentivize over-extraction of residues in deficit regions, potentially encroaching upon the fraction of residue left on field required for SOC maintenance (Brassard et al.,
360 2021; Holmatov et al., 2022). By pinpointing these mismatch hotspots at 1-km resolution, our dataset provides spatially explicit information that can support regional coordination strategies aimed at safeguarding both agroecosystem stability and economic viability.

4.3 Dataset limitations and uncertainty

Although this 1-km dataset provides a mass-balanced representation of residue usage pathways, several sources of
365 uncertainty remain. The primary source of uncertainty stems from assumptions related to livestock feed demand. Current literature exhibits significant variability in these parameters, particularly in dietary intake coefficients for beef cattle (Herrero et al., 2013; Mekonnen and Hoekstra, 2012; Peters et al., 2014; USDA Economic Research Service, 2026). To account for this variability, our study employed scenario analysis to capture the potential range of livestock demands. Across the simulations from S_0 to S_H , the fraction of residues allocated to non-burning pathways (animal and off-field)
370 fluctuated between 5.8% and 27.0%, while the proportion of residues left on field varied from 94.1% to 72.9% (Table S1). This range underscores the sensitivity of residue pathway to livestock management assumptions and highlights the need for more standardized regional feeding parameters. In addition, livestock-associated residue demand was inferred



rather than directly observed, and alternative forage resources such as perennial forages were not explicitly represented, which may influence the magnitude and spatial pattern of inferred residue deficit regions.

375 Another source of uncertainty involves the estimation of off-field residue uses through socio-economic proxies. While international net export data were derived from public records, the estimation of domestic transfers and other off-field uses relies on assumptions. Due to the scarcity of localized empirical data, we utilized a GDP-based proxy to estimate other off-field purposes, calibrated with available U.S.-specific studies (Smerald et al., 2023; Yadav, 2025). Although this approach aligns with previous studies, it remains a simplified representation of real-world complexities. In practice, residue allocation is driven by socio-economic factors such as market price fluctuations, regional policy incentives, and long-term industrial contracts (Downing et al., 2022; Krishna and Mkondiwa, 2023). Our method captures the fundamental spatial patterns of these flows but does not integrate the dynamic socio-economic drivers required to simulate market-driven shifts. Future refinements could incorporate survey-based data to better constrain these parameters against actual market behaviors.

385 Additional uncertainty arises from the representation of residue burning pathways. In this study, a maximum burning fraction of 0.9 was assumed for each grid cell based on published literature (Smerald et al., 2023), and the burning window was defined as the latter portion of the state-level harvest period derived from USDA data (Table 1). While this approach captures the primary post-harvest burning period, some residue burning may occur prior to planting of the subsequent crop, which is not explicitly represented due to data limitations.

390 Finally, uncertainty also remains in the estimation of residue production due to parameter assumptions. Although crop-specific and time-dependent HI were applied, these parameters were assumed to be uniform at the national scale. However, HI can vary across regions due to differences in cultivar choice, management practices, and environmental conditions (Gardner et al., 2021; Pagani et al., 2019). Future work could incorporate region-specific HI parameterization to reduce this uncertainty.

395 **5 Data availability**

The Crop Residue Usage Pathway Dataset (2001–2021) is publicly available from Zenodo at DOI: <https://doi.org/10.5281/zenodo.18453064> (Zhang et al., 2026). The archive provides annual 1-km gridded GeoTIFF layers for the conterminous U.S. for 2001–2021. The dataset contains two components:

(1) **Main products:** including annual scenario-mean (arithmetic mean across four scenarios: S_0 , S_L , S_M , S_H) residue pathway layers (burnt, animal-use, off-field, and left on field), total crop residue production, and arithmetic mean of the mismatched residue.

(2) **Scenario-based products:** intermediate inputs and scenario-specific final outputs. Intermediate input layers include scenario-specific animal-use demand, off-field demand, and mismatch. Scenario-specific final outputs include scenario-specific animal-use, off-field, and residue left on field layers.



405 **6 Conclusions**

This study developed a 1-km gridded dataset linking crop residue production and usage pathways across the conterminous U.S. for 2001-2021. By integrating demand-driven constraints within a mass-balance framework, our dataset provides annual maps of four primary residue pathways, alongside a domestic transfer layer that identifies supply-demand mismatches. The results indicate that residues left on field dominate at the national scale, while animal-use and off-field pathways remain smaller share but spatially heterogeneous. Compared with existing coarse-resolution global products, the 1-km dataset improves geographical fidelity by anchoring estimates to crop pixels and reducing mixed-pixel effects. The mismatch layer further highlights hotspots in the Southeast, West Coast, and the Southern Great Plains, where residue production and demand are spatially separated. Overall, this spatially explicit dataset provides a foundation for evaluating residue production, allocation pathways, and regional supply-demand mismatches, supporting more informed residue management decisions and modeling applications.

7 Acknowledgements

We thank Alan J. Franzluebbers (USDA Agricultural Research Service) and Shuchao Ye (University of Wisconsin–Madison) for their helpful suggestions on manuscript revision and processing of the cropping density dataset.

8 Financial support

420 This work was partly supported by Virginia Tech startup funds and the Virginia Tech Translational Plant Sciences Center Mentee-Faculty Grant.

9 Author contribution

YY conceptualized the study and supervised the project. YZ performed the formal analysis, developed the dataset, and wrote the original draft. YY, YZ, HY, WJ, YK, MS, RS, and BT contributed to reviewing and editing the manuscript.

425 **10 Competing interests**

The contact author has declared that none of the authors has any competing interests.

References

Allmaras, R. R., Schomberg, H. H., Douglas Jr, C. L., and Dao, T. H.: Soil organic carbon sequestration potential of adopting conservation tillage in US croplands, *Journal of Soil and Water Conservation*, 55, 365–373, 2000.



- 430 Anand, A., Kumar, V., and Kaushal, P.: Biochar and its twin benefits: Crop residue management and climate change mitigation in India, *Renewable and Sustainable Energy Reviews*, 156, 111959, 2022.
- Baloch, S. B., Ali, S., Bernas, J., Konvalina, P., Naveed, M., Baloch, F. B., Jamali, Z. H., Lošák, T., Roubík, H., and Ghafoor, A.: Crop Residue Management for Soil Health and Environmental Sustainability: A Comprehensive Review, *Journal of Soil Science and Plant Nutrition*, 25, 7808–7828, 2025.
- 435 Brassard, P., Godbout, S., and Hamelin, L.: Framework for consequential life cycle assessment of pyrolysis biorefineries: a case study for the conversion of primary forestry residues, *Renewable and Sustainable Energy Reviews*, 138, 110549, 2021.
- de Camargo Santos, A., Culman, S. W., and Deiss, L.: Sixty years of crop diversification with perennials improves yields more than no-tillage in Ohio grain cropping systems, *Field Crops Research*, 331, 109993, 2025.
- 440 <https://doi.org/10.1016/j.fcr.2025.109993>, 2025.
- Chatterjee, A.: Annual crop residue production and nutrient replacement costs for bioenergy feedstock production in United States, *Agronomy Journal*, 105, 685–692, 2013.
- Claassen, R., Bowman, M., McFadden, J., Smith, D., and Wallander, S.: Tillage intensity and conservation cropping in the United States, 2018.
- 445 Daioglou, V., Stehfest, E., Wicke, B., Faaij, A., and van Vuuren, D. P.: Projections of the availability and cost of residues from agriculture and forestry, *Gcb Bioenergy*, 8, 456–470, 2016.
- Delandmeter, M., Basso, B., Millar, N., Price, L., Tadiello, T., Rowntree, J., Sacramento, J. P., Sharma, P., Bindelle, J., and Dumont, B.: Boosting ecosystem services and farm economics with crop diversity and livestock integration using a validated modeling approach, *PNAS Nexus*, 4, pgaf377, <https://doi.org/10.1093/pnasnexus/pgaf377>, 2025.
- 450 Downing, A. S., Kumar, M., Andersson, A., Causevic, A., Gustafsson, Ö., Joshi, N. U., Krishnamurthy, C. K. B., Scholtens, B., and Crona, B.: Unlocking the unsustainable rice-wheat system of Indian Punjab: Assessing alternatives to crop-residue burning from a systems perspective, *Ecological Economics*, 195, 107364, 2022.
- Du, Z., Yu, L., Zhao, Y., Li, X., Liu, X., Li, X., Hao, P., Chen, Z., Ma, X., and Wang, H.: Annual global gridded livestock mapping from 1961 to 2021, *Earth System Science Data Discussions*, 2025, 1–20, 2025.
- 455 Eggleston, H. S., Buendia, L., Miwa, K., Ngara, T., and Tanabe, K.: 2006 IPCC guidelines for national greenhouse gas inventories, 2006.
- Farias, G. D., Bremm, C., Lemaire, G., Assmann, T. S., Simões, V. J. L. P., Tiecher, T., Alves, L. A., Martins, A. P., and de Faccio Carvalho, P. C.: Can system fertilization improve plant nutrition and ensure nutrient carryover to successive crops in integrated crop-livestock systems?, *Field Crops Research*, 109985, 2025.
- 460 Fu, B., Chen, L., Huang, H., Qu, P., and Wei, Z.: Impacts of crop residues on soil health: A review, *Environmental Pollutants and Bioavailability*, 33, 164–173, 2021.
- Gardner, A. S., Maclean, I. M. D., Gaston, K. J., and Bütikofer, L.: Forecasting future crop suitability with microclimate data, *Agricultural Systems*, 190, 103084, 2021.
- 465 Garvie, L. C., Lee, D. J., and Kulišić, B.: Towards a Bioeconomy: Supplying Forest Residues for the Australian Market, *Energies*, 17, 397, 2024.



- Gutierrez, S., Grados, D., Møller, A. B., de Carvalho Gomes, L., Beucher, A. M., Giannini-Kurina, F., de Jonge, L. W., and Greve, M. H.: Unleashing the sequestration potential of soil organic carbon under climate and land use change scenarios in Danish agroecosystems, *Science of the Total Environment*, 905, 166921, 2023.
- 470 Haberl, H., Erb, K.-H., Krausmann, F., Loibl, W., Schulz, N., and Weisz, H.: Changes in ecosystem processes induced by land use: Human appropriation of aboveground NPP and its influence on standing crop in Austria, *Global Biogeochemical Cycles*, 15, 929–942, 2001.
- Herrero, M., Havlík, P., Valin, H., Notenbaert, A., Rufino, M. C., Thornton, P. K., Blümmel, M., Weiss, F., Grace, D., and Obersteiner, M.: Biomass use, production, feed efficiencies, and greenhouse gas emissions from global livestock systems, *Proceedings of the National Academy of Sciences*, 110, 20888–20893, 2013.
- 475 Holmatov, B., Schyns, J. F., Krol, M. S., Gerbens-Leenes, P. W., and Hoekstra, A. Y.: Can crop residues provide fuel for future transport? Limited global residue bioethanol potentials and large associated land, water and carbon footprints, *Renewable and Sustainable Energy Reviews*, 149, 111417, 2021.
- Holmatov, B., Hoekstra, A. Y., and Krol, M. S.: EU's bioethanol potential from wheat straw and maize stover and the environmental footprint of residue-based bioethanol, *Mitigation and Adaptation Strategies for Global Change*, 27, 6, 480 2022.
- Hristov, A. N., Johnson, K. A., and Kebreab, E.: Livestock methane emissions in the United States, *Proceedings of the National Academy of Sciences*, 111, E1320–E1320, 2014.
- Jiang, D., Zhuang, D., Fu, J., Huang, Y., and Wen, K.: Bioenergy potential from crop residues in China: Availability and distribution, *Renewable and sustainable energy reviews*, 16, 1377–1382, 2012.
- 485 Karstens, K., Bodirsky, B. L., Dietrich, J. P., Dondini, M., Heinke, J., Kuhnert, M., Müller, C., Rolinski, S., Smith, P., and Weindl, I.: Management-induced changes in soil organic carbon on global croplands, *Biogeosciences*, 19, 5125–5149, 2022.
- Keel, S. G., Hirte, J., Abiven, S., Wüst-Galley, C., and Leifeld, J.: Proper estimate of residue input as condition for understanding drivers of soil carbon dynamics, *Global change biology*, 23, 4455–4456, 2017.
- 490 Krishna, V. V. and Mkondiwa, M.: Economics of crop residue management, *Annual Review of Resource Economics*, 15, 19–39, 2023.
- Kummu, M., Kosonen, M., and Masoumzadeh Sayyar, S.: Downscaled gridded global dataset for gross domestic product (GDP) per capita PPP over 1990–2022, *Scientific Data*, 12, 178, 2025.
- Lal, R.: The Role of Residues Management in Sustainable Agricultural Systems, *Journal of Sustainable Agriculture*, 5, 495 51–78, https://doi.org/10.1300/J064v05n04_06, 1995.
- Lal, R.: World crop residues production and implications of its use as a biofuel, *Environment International*, 31, 575–584, 2005.
- Lehmann, J., Hansel, C. M., Kaiser, C., Kleber, M., Maher, K., Manzoni, S., Nunan, N., Reichstein, M., Schimel, J. P., and Torn, M. S.: Persistence of soil organic carbon caused by functional complexity, *Nature Geoscience*, 13, 529–534, 500 2020.
- Lu, C., Yu, Z., Tian, H., Hennessy, D. A., Feng, H., Al-Kaisi, M., Zhou, Y., Sauer, T., and Arritt, R.: Increasing carbon footprint of grain crop production in the US Western Corn Belt, *Environmental Research Letters*, 13, 124007, 2018.



- 505 McCarty, J. L., Korontzi, S., Justice, C. O., and Loboda, T.: The spatial and temporal distribution of crop residue burning in the contiguous United States, *Science of The Total Environment*, 407, 5701–5712, <https://doi.org/10.1016/j.scitotenv.2009.07.009>, 2009.
- Mekonnen, M. M. and Hoekstra, A. Y.: A global assessment of the water footprint of farm animal products, *Ecosystems*, 15, 401–415, 2012.
- 510 Muth, D. J., Bryden, K. M., and Nelson, R. G.: Sustainable agricultural residue removal for bioenergy: A spatially comprehensive US national assessment, *Applied Energy*, 102, 403–417, <https://doi.org/10.1016/j.apenergy.2012.07.028>, 2013.
- Natalio, A. I., Back, M. A., Richards, A., and Jeffery, S.: Field-scale heterogeneity overrides management impacts following conversion to no-till within an arable system, *Applied Soil Ecology*, 193, 105104, 2024.
- 515 Pagani, V., Guarneri, T., Busetto, L., Ranghetti, L., Boschetti, M., Movedi, E., Campos-Taberner, M., Garcia-Haro, F. J., Katsantonis, D., and Stavrakoudis, D.: A high-resolution, integrated system for rice yield forecasting at district level, *Agricultural systems*, 168, 181–190, 2019.
- Peters, C. J., Picardy, J. A., Darrouzet-Nardi, A., and Griffin, T. S.: Feed conversions, ration compositions, and land use efficiencies of major livestock products in US agricultural systems, *Agricultural Systems*, 130, 35–43, 2014.
- 520 Pongratz, J., Dolman, H., Don, A., Erb, K.-H., Fuchs, R., Herold, M., Jones, C., Kuemmerle, T., Luysaert, S., and Meyfroidt, P.: Models meet data: Challenges and opportunities in implementing land management in Earth system models, *Global change biology*, 24, 1470–1487, 2018.
- Ranaivoson, L., Naudin, K., Ripoche, A., Affholder, F., Rabeharisoa, L., and Corbeels, M.: Agro-ecological functions of crop residues under conservation agriculture. A review, *Agronomy for sustainable development*, 37, 26, 2017.
- Röder, M., Chong, K., and Thornley, P.: The future of residue-based bioenergy for industrial use in Sub-Saharan Africa, *Biomass and Bioenergy*, 159, 106385, 2022.
- 525 Russelle, M. P., Entz, M. H., and Franzluebbers, A. J.: Reconsidering integrated crop–livestock systems in North America, *Agronomy journal*, 99, 325–334, 2007.
- Scarlat, N., Martinov, M., and Dallemand, J.-F.: Assessment of the availability of agricultural crop residues in the European Union: Potential and limitations for bioenergy use, *Waste management*, 30, 1889–1897, 2010.
- 530 Schmer, M. R., Brown, R. M., Jin, V. L., Mitchell, R. B., and Redfearn, D. D.: Corn residue use by livestock in the United States, *Agricultural & Environmental Letters*, 2, 160043, 2017.
- van Selm, B., Hijbeek, R., van Middelaar, C. E., de Boer, I. J., and van Ittersum, M. K.: How to use residual biomass streams in circular food systems to minimise land use or GHG emissions, *Agricultural Systems*, 222, 104185, 2025.
- Smerald, A., Rahimi, J., and Scheer, C.: A global dataset for the production and usage of cereal residues in the period 1997–2021, *Scientific data*, 10, 685, 2023.
- 535 Smil, V.: Crop Residues: Agriculture’s Largest Harvest: Crop residues incorporate more than half of the world’s agricultural phytomass, *Bioscience*, 49, 299–308, 1999.
- Sulc, R. M. and Tracy, B. F.: *Integrated crop–livestock systems in the US Corn Belt*, Wiley Online Library, 2007.



- Taifouris, M. and Martín, M.: Integrating intensive livestock and cropping systems: sustainable design and location, *Agricultural Systems*, 203, 103517, 2022.
- 540 Tian, H., Lu, C., Yang, J., Banger, K., Huntzinger, D. N., Schwalm, C. R., Michalak, A. M., Cook, R., Ciais, P., and Hayes, D.: Global patterns and controls of soil organic carbon dynamics as simulated by multiple terrestrial biosphere models: Current status and future directions, *Global Biogeochemical Cycles*, 29, 775–792, 2015.
- Tittonell, P., Gérard, B., and Erenstein, O.: Tradeoffs around crop residue biomass in smallholder crop-livestock systems—What’s next?, *Agricultural systems*, 134, 119–128, 2015.
- 545 Umakanth, A. V., Datta, A., Reddy, B. S., and Bardhan, S.: Biomass feedstocks for advanced biofuels: sustainability and supply chain management, *Advanced biofuel technologies*, 39–72, 2022.
- USDA Economic Research Service: Cattle & Beef: Sector at a Glance. <https://www.ers.usda.gov/topics/animal-products/cattle-beef/sector-at-a-glance>, 2025.
- 550 Wang, M., Wan, D., Xie, X., Bai, Z., Wang, R., Zhang, X., Gao, Y.-Z., Tan, Z., and Yin, Y.: Crop-livestock integration: Implications for food security, resource efficiency and greenhouse gas mitigation, *Innovation Life*, 2, 10.59717, 2024.
- Wanjura, J. D., Faulkner, W. B., Barnes, E. M., Holt, G. A., and Pelletier, M. G.: Crop residue inventory estimates for Texas High Plains cotton, in: *Proc. Beltwide Cotton Conf.*, Orlando, FL, 3–6, 2012.
- Weldesemayat Sileshi, G., Barrios, E., Lehmann, J., and Tubiello, F. N.: An organic matter database (OMD): consolidating global residue data from agriculture, fisheries, forestry and related industries, *Earth System Science Data*, 17, 369–391, 2025.
- 555 Wiedinmyer, C., Kimura, Y., McDonald-Buller, E. C., Emmons, L. K., Buchholz, R. R., Tang, W., Seto, K., Joseph, M. B., Barsanti, K. C., and Carlton, A. G.: The Fire Inventory from NCAR version 2.5: an updated global fire emissions model for climate and chemistry applications, *Geoscientific Model Development*, 16, 3873–3891, 2023.
- 560 Xing, J., Song, J., Liu, C., Yang, W., Duan, H., Yabar, H., and Ren, J.: Integrated crop–livestock–bioenergy system brings co-benefits and trade-offs in mitigating the environmental impacts of Chinese agriculture, *Nature Food*, 3, 1052–1064, 2022.
- Yadav, V.: From Waste to Resource: Advancing Sustainable Crop Residue Management Globally, *International Journal of Research and Review*, <https://doi.org/10.52403/ijrr.20250578>, 2025.
- 565 Ye, S., Cao, P., and Lu, C.: Annual time-series 1 km maps of crop area and types in the conterminous US (CropAT-US): cropping diversity changes during 1850–2021, *Earth System Science Data*, 16, 3453–3470, 2024.
- Yu, Z. and Lu, C.: Historical cropland expansion and abandonment in the continental US during 1850 to 2016, *Global Ecology and Biogeography*, 27, 322–333, 2018.
- Zeng, N., Zhao, F., Collatz, G. J., Kalnay, E., Salawitch, R. J., West, T. O., and Guanter, L.: Agricultural Green Revolution as a driver of increasing atmospheric CO₂ seasonal amplitude, *Nature*, 515, 394–397, 2014.
- 570 Zhang, J., Zhuge, C., Huang, Q., Wang, B., Li, Y., and Oosterveer, P.: Farmers’ decisions on crop residues utilization, greenhouse gases reduction and subsidy of crop residue-based bioenergy: An agent-based life cycle model, *Sustainable Production and Consumption*, 55, 24–36, <https://doi.org/10.1016/j.spc.2025.02.001>, 2025.

<https://doi.org/10.5194/essd-2026-237>
Preprint. Discussion started: 29 April 2026
© Author(s) 2026. CC BY 4.0 License.



575 Zhang, Y., Yan, H., Jiao, W., Kang, Y., Schmer, M. R., Stewart, R. D., Tracy, B. F., & You, Y. (2026). Crop Residue Pathway Dataset_v1 [Data set]. Virginia Tech, School of Plant and Environmental Sciences. <https://doi.org/10.5281/zenodo.18453064>